

# Yip1A regulates the COPI-independent retrograde transport from the Golgi complex to the ER

Fumi Kano<sup>1,2</sup>, Shinobu Yamauchi<sup>1,\*</sup>, Yumi Yoshida<sup>3</sup>, Miho Watanabe-Takahashi<sup>4</sup>, Kiyotaka Nishikawa<sup>4</sup>, Nobuhiro Nakamura<sup>3</sup> and Masayuki Murata<sup>1,‡</sup>

<sup>1</sup>Department of Life Sciences, Graduate School of Arts and Sciences, The University of Tokyo, Komaba 3-8-1, Meguro-ku, Tokyo 153-8902, Japan

<sup>2</sup>PRESTO, Japan Science and Technology Agent, 4-1-8 Honcho Kawaguchi, Saitama, Japan

<sup>3</sup>Division of Life Sciences, Graduate School of Natural Science and Technology and Faculty of Pharmaceutical Sciences, Kanazawa University, Kakuma, Kanazawa 920-1192, Japan

<sup>4</sup>Faculty of Life and Medical Science, Doshisha University, Kyoto 610-0394, Japan

\*Present address: Dokkyo University, Gakuen-cho 1-1, Soka, Saitama 340-0042, Japan

‡Author for correspondence (e-mail: mmurata@bio.c.u-tokyo.ac.jp)

Accepted 19 March 2009

Journal of Cell Science 122, 2218-2227 Published by The Company of Biologists 2009

doi:10.1242/jcs.043414

## Summary

**Yip1A, a mammalian homologue of yeast Yip1p, is a multi-spanning membrane protein that is considered to be involved in transport between the endoplasmic reticulum (ER) and the Golgi. However, the precise role of Yip1A in mammalian cells remains unclear. We show here that endogenous Yip1A is localized to the ER-Golgi intermediate compartment (ERGIC). Knockdown of Yip1A by RNAi did not induce morphological changes in the Golgi, ER, or ERGIC. By analyzing a number of intracellular transport pathways, we found that Yip1A knockdown delayed the transport of Shiga toxin from the Golgi to the ER, but did not affect the anterograde transport of VSVGts045. We also found that a recombinant protein that corresponded to the N-terminal domain of Yip1A inhibited the**

**COPI-independent retrograde transport of GFP-tagged galactosyltransferase, GT-GFP, but not the COPI-dependent retrograde transport of p58/ERGIC53. Furthermore, we found that Yip1A knockdown resulted in the dissociation of Rab6 from the membranes. These results suggested that Yip1A has a role in COPI-independent retrograde transport from the Golgi to the ER and regulates the membrane recruitment of Rab6.**

Supplementary material available online at <http://jcs.biologists.org/cgi/content/full/122/13/2218/DC1>

Key words: Retrograde transport, Yip1A, Golgi complex, Endoplasmic reticulum

## Introduction

The endoplasmic reticulum (ER) and the Golgi complex both maintain their specific morphology, composition and function in spite of the exchange of proteins and lipids between the two organelles through vesicular transport. The morphology of the Golgi complex is closely linked to the balance between anterograde (ER-to-Golgi) and retrograde (Golgi-to-ER) transport. It has been reported that the inhibition of anterograde transport leads to the redistribution of Golgi components to the cytoplasm or the ER (Storrie et al., 1998; Ward et al., 2001; Miles et al., 2001). Inhibition of anterograde transport at the onset of mitosis also results in the relocation of Golgi enzymes to the ER (Zaal et al., 1999; Altran-Bonnet et al., 2006), although it is controversial as to whether the Golgi mixes with the ER or whether they remain separate throughout mitosis (Lowe and Barr, 2007). Thus, the rates of anterograde and retrograde transport between the two organelles appear to be strictly regulated in living cells.

The molecular mechanisms that underlie anterograde and retrograde transport between the ER and the Golgi have been studied for decades, and it is known that several types of small GTPase have crucial roles in different steps of the transport pathways. In anterograde transport from the ER to the Golgi, the GTP-bound form of Sar1, which is a small GTPase, initiates COPII coat assembly on the ER membrane and COPII vesicles bud from the ER to deliver the cargo to the Golgi (Kuge et al., 1994; Springer et al., 1999; Sato and Nakano, 2007). In retrograde transport from the Golgi to the ER, ARF, which is another small GTPase, recruits the coatamer protein complex to the Golgi membrane to form COPI

vesicles (Serafini et al., 1991; Gaynor et al., 1998; Bremser et al., 1999), although several cargo proteins, which include Shiga toxin (Stx) and the Golgi enzymes, are transported from the Golgi to the ER in a COPI-independent manner (Girod et al., 1999). Another important type of small GTPase that has crucial roles in the vesicular transport between the two organelles is the Rab GTPase family. Rab proteins are active in their GTP-bound form, they are recruited to specific membranes by their binding partners, and they promote cargo selection, vesicle budding, tethering, and fusion processes (Grosshans et al., 2006).

One group of proteins that could regulate the membrane association of the Rab proteins is the Yip family. Members of the Yip family have a hydrophilic N-terminal domain and a hydrophobic multi-membrane spanning C-terminal domain, and are conserved in eukaryotes. They bind to Rab proteins in a prenylation-dependent manner and can associate with other Yip proteins (Calero et al., 2002; Calero et al., 2003; Shakoori et al., 2003). Sivars and colleagues (Sivars et al., 2003) found that Yip3, a Yip family protein, dissociates the complex between Rab9 and Rab-GDI and delivers Rab9 to endosomal membranes. The results of this study and others (Chen and Collins, 2005) indicate that Yip proteins could regulate the recruitment of Rab proteins to their cognate membranes. One member of the Yip family in yeast, Yip1p, is essential for growth and interacts with different di-prenylated Rabs with varying affinities (Calero et al., 2003; Yang et al., 1998). An accumulation of ER membranes and defects in secretion were observed in a Yip1 mutant (Yang et al., 1998), and an anti-Yip1p antibody inhibited COPII vesicle budding in vitro (Heidtmann et al., 2003), and also

affected the fusion competence of ER-derived vesicles (Barrowman et al., 2003). These results indicate that Yip1p is involved in anterograde transport from the ER to the Golgi.

Although human Yip1A (official symbol YIPF5) can rescue the Yip1 mutant, little is known about the function of mammalian Yip1A. Yip1A is a transmembrane protein that localizes to the Golgi and to ER-exit sites (ERES) (Tang et al., 2001), and to the ER-Golgi intermediate compartment (ERGIC) (Yoshida et al., 2008). Tang and co-workers (Tang et al., 2001) demonstrated that Yip1A binds to Sec23 and Sec24, which are components of COPII vesicles, and that overexpression of the soluble N-terminal domain of Yip1A arrests the transport of VSVGts045, which is a temperature-sensitive mutant of vesicular stomatitis virus G (VSVG) protein and a marker of vesicular transport, not in the ER network, but at the juxtannuclear region. Yip1A also interacts with Yif1, another member of the Yip family, and localizes Yif1 to the Golgi complex (Jin et al., 2005). Thus, the function and localization of mammalian Yip1A are still controversial.

In this study, we raised a polyclonal antibody against a soluble N-terminal peptide of Yip1A, and investigated the localization of endogenous Yip1A. We also examined the effect of Yip1A knockdown by RNA interference (RNAi) on the morphology of various organelles that are involved in vesicular transport. In addition, we assessed the role of Yip1A in different transport pathways and found that Yip1A has a role in COPI-independent retrograde transport from the Golgi to the ER by regulating the membrane association of Rab6.

## Results

### Yip1A localizes to the ERGIC

We generated rabbit polyclonal antibodies against several mouse Yip1A peptides, and found that one of these antibodies, which was directed against the peptide that encodes amino acids 35-54 of mouse Yip1A, could recognize endogenous Yip1A in HeLa cells (Fig. 1A, control RNAi) and CHO cells (F.K., unpublished). We performed dual immunofluorescence analysis using our anti-Yip1A antibody and antibodies against various organelle markers (ERGIC53 for the ERGIC, GM130 for the *cis*-Golgi, p230 for the *trans*-Golgi, and Sec31A for the ERES) (Fig. 1C; supplementary material Fig. S1A), and found that Yip1A colocalized extensively with ERGIC53 (Fig. 1C). In addition, Yip1A within the cytoplasmic punctate structures colocalized with Sec31A, the marker for the ERES (supplementary material Fig. S1A, Sec31A). Hammond and Glick (Hammond and Glick, 2000) also reported the close colocalization of ERGIC53 with COPII. By contrast, neither GM130 nor p230 completely colocalized with Yip1A (supplementary material Fig. S1A, GM130 and p230). We found that, in HeLa cells treated with 5  $\mu$ g/ml brefeldin A (BFA) for 30 minutes, the endogenous Yip1A remained in punctate structures throughout the cytoplasm and these structures were stained with ERGIC53 (F.K., unpublished). These results indicated that endogenous Yip1A, which was detected by immunofluorescence using our antibody, localizes to the ERGIC. We also observed bright staining at the centrosome (Fig. 1A, control RNAi, and Fig. 1C, Yip1A). However, the fluorescent signal around the centrosome area was not affected by knockdown of Yip1A by RNAi (Fig. 1A, Yip1A RNAi), which suggested that the signal at the centrosome might be due to non-specific staining by the antibody. We confirmed by western blotting that the amount of Yip1A protein was reduced to approximately 18% of the normal level by gene silencing of Yip1A (Fig. 1B).

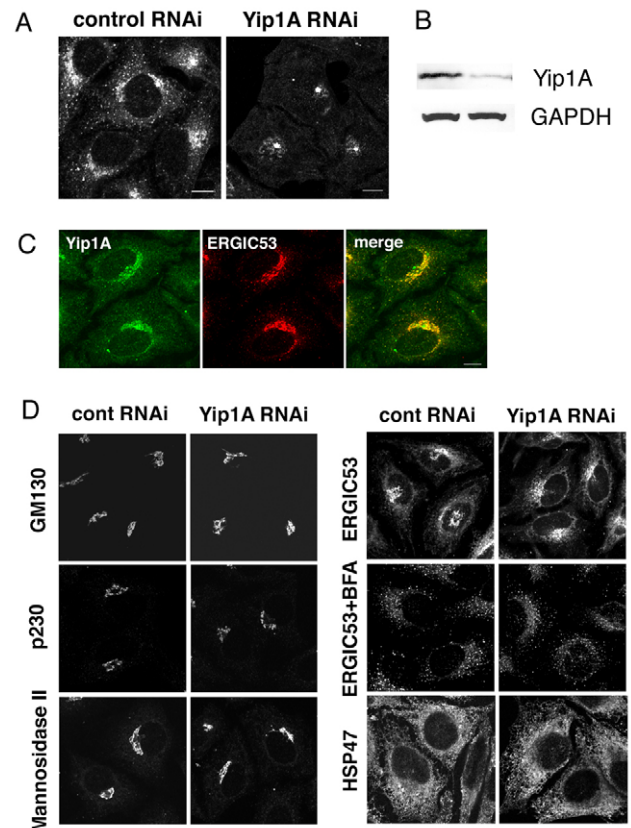


**Fig. 1.** Endogenous Yip1A is localized to the ERGIC in HeLa cells. HeLa cells were transfected with a scrambled siRNA (control RNAi) or an siRNA against Yip1A (Yip1A RNAi). (A) After 72 hours, the cells were immunostained with the anti-Yip1A antibody. (B) Cells were lysed 72 hours after siRNA transfection, and were subjected to western blotting using the anti-Yip1A or anti-GAPDH antibody. (C) HeLa cells were fixed and immunostained using the anti-Yip1A antibody and antibodies against ERGIC53. Scale bars: 10  $\mu$ m. (D) Control or Yip1A-knockdown HeLa cells were immunostained with antibodies against GM130, p230, mannosidase II, ERGIC53, and HSP47. For ERGIC53+BFA, control or Yip1A, siRNA-transfected cells were treated with 5  $\mu$ g/ml BFA at 37°C for 30 minutes, and then immunostained with the anti-ERGIC53 antibody.

Knockdown of Yip1A by RNAi did not induce morphological changes within the ER, Golgi or ERGIC

To investigate the effect of Yip1A on the maintenance of different organelles, we examined the morphologies of various organelles in Yip1A-knockdown cells. An siRNA against human Yip1A was transfected into HeLa cells, and after a 72-hour incubation, the cells were immunostained with antibodies against various organelle markers. We used antibodies against GM130, p230 and mannosidase II to identify the Golgi, antibodies against ERGIC53 and p115 for the ERGIC, an antibody against HSP47 together with ER tracker Blue-White DPX dye for the ER, an antibody against  $\beta$ COP for COPI vesicles, and an antibody against Sec31A for COPII vesicles. As shown in Fig. 1D and supplementary material Fig. S1B, the localization of these organelle markers was almost unchanged in Yip1A-knockdown cells compared with control cells. In most cases, the Golgi in the Yip1A-knockdown cells showed a normal perinuclear structure; however, some fragmented Golgi were observed in the cells.

### Investigation of the involvement of Yip1A in different transport pathways by RNAi

To examine the effect of gene silencing of Yip1A on vesicular transport pathways, we assayed the anterograde transport of VSVG from the ER to the plasma membrane via the Golgi, and the retrograde transport of Shiga toxin (Stx) from the plasma membrane to the ER via the Golgi in Yip1A-knockdown cells.

The kinetics of VSVGts045 transport from the ER to the Golgi were measured in Yip1A-knockdown cells. The extent of VSVGts045-GFP transport for each incubation time was estimated by both morphometric analysis (Fig. 2A,B) and the resistance to endoglycosidase-H (endo-H) (supplementary material Fig. S2A). The kinetics of VSVG transport were indistinguishable between the control and Yip1A-knockdown cells (Fig. 2B; supplementary material Fig. S2A). These results indicated that Yip1A was not involved in the anterograde transport of VSVG from the ER to the plasma membrane.

We then investigate the transport of Stx from the plasma membrane to the ER in control or Yip1A-knockdown cells by morphometric analysis. In control cells, Stx-Cy2 that had bound to cell surface receptors was endocytosed and transported to the endosomal structures within 1 hour (Fig. 2C, endosome). These structures were confirmed as endosomes by dual immunostaining with an antibody against EEA1, an early endosome marker protein, (M.T., unpublished results). The endocytosed Stx-Cy2 was further transported to the Golgi complex (Fig. 2C, Golgi) within 2 hours, and finally reached the ER network within 3-5 hours (Fig. 2C, ER). As shown in Fig. 2D (Golgi), the delivery of Stx-Cy2 from the plasma membrane to the Golgi in Yip1A-knockdown cells showed the same kinetics as the control cells (Fig. 2D, Golgi, 0-1 hour). After 1 hour of incubation, the amount of Stx that was accumulated in the Golgi decreased gradually, which suggested that retrograde transport of Stx from the Golgi to the ER had occurred. It should be noted that this decrease occurred more slowly in the Yip1A-knockdown cells than in the control cells (Fig. 2D, Golgi and ER, 1-5 hours). These results indicated that knockdown of Yip1A in HeLa cells affected the later stage of retrograde transport of Stx (from the Golgi to the ER) but had no effect on its earlier stage (from the plasma membrane to the Golgi via endosomes). To confirm the morphometric results, we examined the rate of cell death by Stx catalytic subunits that had been translocated from the ER luminal side to the cytoplasm and had inhibited the protein synthesis. As shown in supplementary material Fig. S2B, the rate of cell death due to Stx was also slower in the Yip1A-knockdown cells than in the control cells.

We also investigated the retrograde transport of cation-independent mannose-6-phosphate receptor that had been tagged with GFP (GFP-CI-MPR) in Yip1A-knockdown cells by FRAP (fluorescence recovery after photobleaching). The kinetics of fluorescence recovery at the juxtannuclear region in the Yip1A-knockdown cells were indistinguishable from those in the control cells (supplementary material Fig. S3), indicating that Yip1A is not involved in the retrograde transport of GFP-CI-MPR from the endosomes to the Golgi.

### Regulation of Rab6 recruitment to the Golgi membranes by Yip1A

We focused on the localization of the Golgi-associated Rab proteins, Rab6, Rab1b and Rab33b, in Yip1A-knockdown cells. These Rab GTPases have crucial roles in vesicular transport between organelles (Girod et al., 1999; White et al., 1999; Grigoriev et al., 2007; Allan

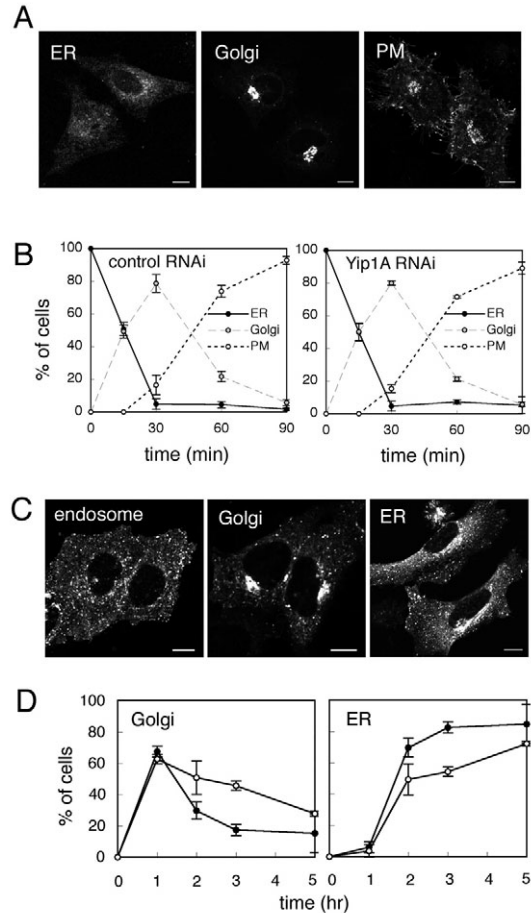


**Fig. 2.** Transport assays for VSVG and Stx in Yip1A-knockdown cells. (A) Representative images of the cells in which VSVGts045-GFP was localized to the ER, to the Golgi and to the plasma membrane (PM). Scale bars: 10  $\mu$ m. (B) Kinetics of VSVGts045 transport in control or Yip1A-knockdown HeLa cells. The graph shows the mean percentage of cells ( $\pm$  s.d.) in which VSVGts045-GFP was localized to the ER, the Golgi or the plasma membrane (PM).  $n=300$ . (C) Representative images of the cells in which Cy2-labelled Stx was localized to the endosomes, to the Golgi, and to the ER. Scale bars: 10  $\mu$ m. (D) Kinetics of Stx transport in control or Yip1A-knockdown HeLa cells. The mean percentage of cells ( $\pm$  s.d.) in which Stx had accumulated in the Golgi or arrived at the ER is shown in the graph. Filled and open circles represent the control and Yip1A-knockdown cells, respectively.  $n=300$ .

et al., 2000; Saraste et al., 1995; Plutner et al., 1991; Tisdale et al., 1992; Zheng et al., 1998; Valsdottir et al., 2001; Jiang and Storrie, 2005).

Gene silencing of Yip1A by RNAi was performed in HeLa cells. After 72 hours, the presence of Rab6, Rab1b and Rab33b in the membrane fraction and in the total cell lysate was determined and quantified by western blotting. Membrane fractions of cells were prepared according to the method described by Lawe and colleagues (Lawe et al., 2003). As shown in Fig. 3A,B, the level of membrane-associated Rab6 in Yip1A-knockdown cells decreased to 51.9% of that in the control, whereas the levels of membrane-associated Rab1b and Rab33b were 85.8% and 99.6%, respectively, of that in the control. We also confirmed that there was no reduction in total Rab6, Rab1b or Rab33b protein in Yip1A-knockdown cells compared with control cells (supplementary material Fig. S4). Next,

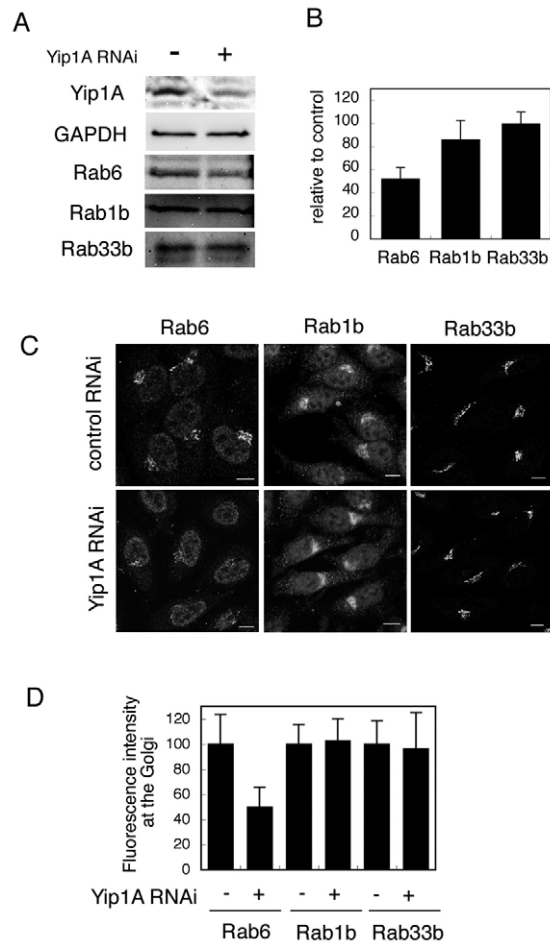


**Fig. 3.** Rab6, but not Rab1b or Rab33b, dissociates from membranes in Yip1A-knockdown cells. (A) The amount of Yip1A and GAPDH or membrane-associated Rab6, Rab1b and Rab33b in control (Yip1A RNAi<sup>-</sup>) or Yip1A-knockdown (Yip1A RNAi<sup>+</sup>) cells was quantified by western blotting. Protein levels were normalized against the protein concentration of the cytosolic fraction. (B) The percentage of Rab6, Rab1b and Rab33b in the membrane fraction in Yip1A-knockdown cells was calculated relative to the amount in the control cells, and the means  $\pm$  s.d. from three independent experiments are shown. (C) Control or Yip1A-knockdown HeLa cells were fixed and stained with anti-Rab6, anti-Rab1b, or anti-Rab33b antibodies. Scale bars: 10  $\mu$ m. (D) The relative percentage of fluorescence intensity of Rab6, Rab1b, or Rab33b in the Golgi was measured in control (RNAi<sup>-</sup>) or Yip1A-knockdown (RNAi<sup>+</sup>) HeLa cells.

we examined the changes in localization of Rab6, Rab1b and Rab33b in control and Yip1A-knockdown cells by immunofluorescence. In control cells, Rab6 was observed in the Golgi region (Fig. 3C, Rab6 control RNAi). In Yip1A-knockdown cells, the fluorescence intensity of Rab6 in the Golgi region decreased to 49.7% and appeared to become blurred compared with that in control cells (Fig. 3C,D). By contrast, Rab1b was localized to the Golgi region and cytoplasmic vesicles, and its localization and fluorescence intensity were almost identical in control and knockdown cells (Fig. 3C,D, Rab1b). In addition, knockdown of Yip1A did not affect the localization of Rab33b to the Golgi (Fig. 3C,D, Rab33b). These results indicated that Yip1A knockdown induced the dissociation, probably from the Golgi membranes, of Rab6, but not Rab1b or Rab33b. We also tried to investigate the

effect of Yip1A knockdown on the localization of Rab1a and Rab2, which are other Golgi-associated Rab proteins. However, unfortunately, we detected non-specific staining of cytoplasmic membranous structures or microtubules by the anti-Rab1a and anti-Rab2 antibodies, which made it impossible to estimate the amount of Golgi-associated Rab1a and Rab2.

#### Soluble N-terminal peptides of Yip1A inhibited COPI-independent retrograde transport but not anterograde transport

It has been reported that there are at least two different pathways of retrograde transport from the Golgi to the ER: the COPI-dependent and COPI-independent pathways. Rab6 was found to regulate specifically the COPI-independent transport pathway (Girod et al., 1999), which includes the Golgi-to-ER transport of Stx. We investigated whether Yip1A is involved in the COPI-independent pathway alone or in both the COPI-dependent and -independent pathways. To this end, we used two types of reconstitution assay for retrograde transport: one measures the transport of GT-GFP, which comprises the first 60 amino acids of galactosyltransferase fused with GFP and is known to cycle between the ER and the Golgi (Zaal et al., 1999) in a COPI-independent manner, and the other measures the transport of GFP-tagged p58, which is a rat homologue of ERGIC53 that is known to be transported from the ERGIC to the ER in a COPI-dependent manner (Girod et al., 1999).

At first, we tried to use HeLa-GT cells, which stably express GT-GFP, for the retrograde transport assay, but we could not isolate suitable HeLa-GT cell lines for the FRAP experiment. So we used CHO-GT8 cells (Kano et al., 2000), which express GT-GFP stably, and applied FRAP to compare quantitatively the extent of the transport of GT-GFP under various conditions in CHO-GT8 cells (see Materials and Methods).

For the assay, semi-intact CHO-GT8 cells were incubated with cytosol and the ATP regenerating system (cytosol and ATP). The morphology of the ER region in which fluorescence recovery was measured resembled that of the region before bleaching, and GT-GFP signal was distributed in the characteristic ER network configuration, which is connected by three-way junctions, after the assay (Fig. 4A; supplementary material Fig. S5A). The fluorescent network that could initially be recovered, was continuous, which was confirmed by the complete bleach upon repeated illumination (F.K., unpublished results). In addition, fluorescence recovery in the ER region was not due to the appearance of newly synthesized GT-GFP because when both the Golgi and ER regions were photobleached simultaneously, no fluorescence recovery was observed in the ER region (F.K., unpublished results). Fig. 4B shows representative kinetics curves for fluorescence recovery within the bleached ER region. Approximately 25–30% of the fluorescence intensity was recovered in the presence of cytosol and ATP (Fig. 4B, cytosol+ATP). In the presence of ATP alone or cytosol that contained GTP $\gamma$ S, under which conditions retrograde transport is inhibited (Hidalgo et al., 1995), fluorescence recovery within the bleached ER region was reduced to less than 10% (Fig. 4B, ATP and GTP $\gamma$ S). The retrograde transport of GT-GFP required the addition of cytosol with a protein concentration of at least 2.5 mg/ml, together with the hydrolysis of ATP and GTP (supplementary material Fig. S5B, cytosol+ATP, ATP, AMP-PNP and GTP $\gamma$ S). Depolymerization of microtubules by treatment with nocodazole as described (Kano et al., 2000) resulted in the complete inhibition of transport (supplementary material Fig. S5B, nocodazole). This

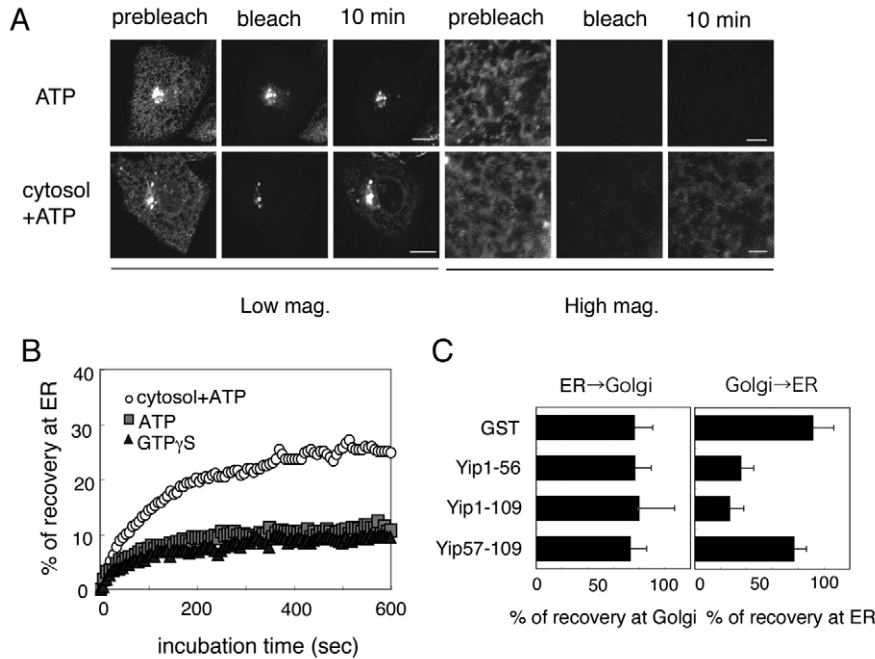


**Fig. 4.** Reconstitution of retrograde transport of GT-GFP: Yip1-56 and Yip1-109 inhibited the COPI-independent retrograde transport of GT-GFP. (A) CHX-treated, semi-intact CHO-GT8 cells were incubated with an ATP-regenerating system only (ATP) or cytosol and ATP (cytosol+ATP), and subjected to the retrograde transport assay. The cells were viewed at low or high magnification. Scale bars: 10  $\mu$ m (Low mag.) or 2  $\mu$ m (High mag.). (B) Kinetics of fluorescence recovery after photobleaching in the ER region in the presence of cytosol and ATP (cytosol+ATP), an ATP-regenerating system only (ATP), or cytosol and ATP plus 1 mM GTP $\gamma$ S (GTP $\gamma$ S). (C) Anterograde and retrograde transport assays were performed in the presence of rat liver cytosol, an ATP-regenerating system, and 5  $\mu$ g GST, Yip1-56, Yip1-109 or Yip57-109. The mean percentage ( $\pm$  s.d.) of fluorescence recovery in the Golgi (anterograde) or the ER (retrograde) is shown in the graph.

was not consistent with the result described by Storrie and co-workers (Storrie et al., 1998), who showed that VSV-tagged N-acetylgalactosaminyltransferase-2 (GalNAc-T2-VSV) accumulated gradually in the ER in Sar1H79G-expressing, nocodazole-treated cells. We suppose that disruption of the microtubules can affect retrograde transport but that intact microtubules are not essential for the process. Therefore, although we detect the inhibition of transport by nocodazole treatment during the 10-minute incubation period in our transport assay, GalNAc-T2-VSV might be able to relocate to the ER over a longer time period. Another possibility is that the difference in microtubule requirements could be due to in part to comparing an *in vitro* semi-intact cell system with an experiment performed in intact cells. There might be more redundant pathways in intact cells for retrograde trafficking.

We also found that, although the addition of recombinant protein of Sar1T39N, which is a GDP-restricted mutant of Sar1 and had been used to block COPII-dependent trafficking (Zaal et al., 1999; Ward et al., 2001; Stroud et al., 2003), inhibited anterograde transport (supplementary material Fig. S6E, Sar1T39N), it did not affect the measurements that were obtained for retrograde transport (supplementary material Fig. S5C, Sar1T39N). This result indicated that the fluorescence recovery in the ER region in our retrograde transport assay was attributable solely to the retrograde transport of GT-GFP from the Golgi to the ER, and not to anterograde transport from the ER.

We prepared recombinant proteins that consisted of the N-terminal amino acids 1-56, 1-109 or 57-109 of Yip1A fused with GST (referred to as Yip1-56, Yip1-109 and Yip57-109, respectively) and examined their effects on the retrograde transport. We used rat liver cytosol for the following experiments because of its high protein concentration (~15 mg/ml). Rat liver cytosol had a similar ability to reconstitute vesicular trafficking in semi-intact cells as L5178Y cytosol (F.K., unpublished). Semi-intact CHO-GT8 cells were incubated with rat liver cytosol and 5  $\mu$ g Yip1-56, Yip1-109, or Yip57-109, and then subjected to the transport assay. As shown in Fig. 4C, retrograde transport was inhibited by the addition of Yip1-56 or Yip1-109 (Fig. 4C, Golgi→ER, Yip1-56 and Yip1-109),

but not by Yip57-109 (Fig. 4C, Golgi→ER, Yip57-109). Therefore, we supposed that the soluble N-terminal peptides inhibit the retrograde transport of GT-GFP in a competitive manner and that the first 56 amino acids of Yip1A are sufficient for the inhibition. We did not observe any inhibitory effect of anti-Yip1A antibody on the retrograde transport.

We could also reconstitute the anterograde transport of GT-GFP in semi-intact cells in the same manner (described in detail in supplementary material Fig. S6), and found that the transport was dependent on cytosol, hydrolysis of nucleotides, microtubule integrity, and COP II vesicles (supplementary material Fig. S6D). Interestingly, the soluble N-terminal peptides of Yip1A had no effect on the anterograde transport (Fig. 4C, ER→Golgi). The kinetics of fluorescence recovery in the presence or absence of the Yip1A peptides were identical (supplementary material Fig. S7), and we did not observe any accumulation of intermediary structures in the presence of these peptides.

#### The soluble N-terminal peptides of Yip1A had no effect on COPI-dependent retrograde transport

Next, we investigated the effect of Yip1-56 and Yip1-109 on the retrograde transport of p58. It has been reported that p58 relocates to the ER in a COPI-dependent manner when anterograde transport is arrested by GTP-restricted Sar1 mutant protein (Girod et al., 1999). To reconstitute the retrograde transport of p58, we established a stable cell line, CHO-p58, in which GFP-tagged p58 is continuously expressed. GFP-p58 was observed, in CHO-p58 cells, in the juxtannuclear region and punctate structures that were scattered throughout the cytoplasm. These observations were consistent with immunofluorescence images that were obtained using an anti-ERGIC53 antibody (F.K., unpublished). To confirm that the retrograde transport of p58 in the assay is COPI dependent, we made use of an anti- $\beta$ COP antibody. Microinjection of a monoclonal anti- $\beta$ COP antibody that is directed against a synthetic peptide that encodes amino acids 496-513 of  $\beta$ COP has been reported to inhibit almost completely the ER-to-Golgi transport of VSVG in tubular membranes (Pepperkok et al., 1993). We used the same peptide

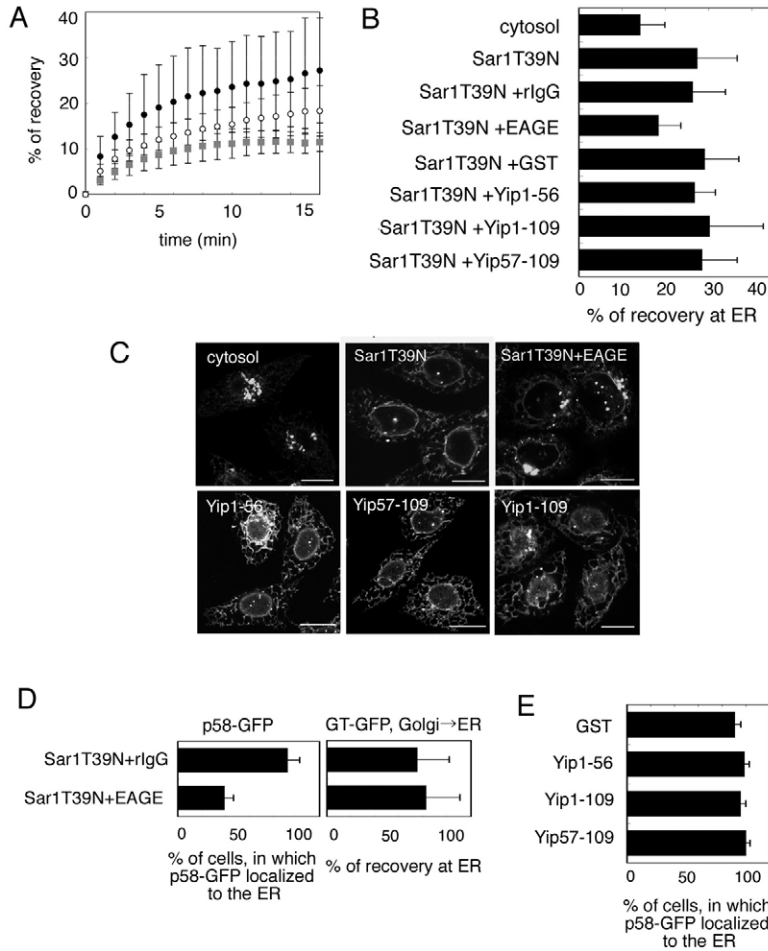


**Fig. 5.** Yip1A 1-56 and 1-109 did not inhibit the COPI-dependent retrograde transport of p58. (A) Kinetics of fluorescence recovery of GFP-p58 in the ER region in the presence of rat liver cytosol (grey squares); cytosol and 5  $\mu$ g Sar1T39N (black circles); or cytosol, Sar1T39N and 5  $\mu$ g anti-EAGE2 antibody (white circles). (B) CHX-treated, semi-intact CHO-p58 cells were incubated with cytosol; cytosol and 5  $\mu$ g Sar1T39N; cytosol, Sar1T39N and 5  $\mu$ g rabbit IgG (rlgG); cytosol, Sar1T39N and 5  $\mu$ g anti-EAGE2 antibody (EAGE); cytosol, Sar1T39N and 5  $\mu$ g GST; or cytosol, Sar1T39N and 5  $\mu$ g of the following Yip peptides: Yip1-56, Yip1-109 or Yip57-109. GFP-p58 in the ER region was bleached and the percentages of fluorescence recovery in the ER at 15 minutes after bleaching are shown in the graph. (C) Semi-intact CHO-p58 cells were incubated with rat liver cytosol; cytosol and 5  $\mu$ g Sar1T39N; cytosol, Sar1T39N and 5  $\mu$ g anti-EAGE2 antibody; cytosol, Sar1T39N and 5  $\mu$ g Yip1-56, Yip1-109 or Yip57-109 at 32°C for 1 hour. The cells were fixed and viewed by confocal microscopy. Scale bars: 10  $\mu$ m. (D) Semi-intact CHO-p58 or semi-intact CHO-GT cells were incubated with control rabbit IgG or anti-EAGE2 antibody in the presence of rat liver cytosol and 5  $\mu$ g Sar1T39N. The cells were then subjected to the retrograde transport assay for GFP-p58 and GT-GFP. (E) Semi-intact CHO-p58 cells were incubated with GST, Yip1-56, Yip1-109 or Yip57-109 in the presence of rat liver cytosol and 5  $\mu$ g Sar1T39N protein, and then were subjected to the retrograde transport assay for GFP-p58. All results are means  $\pm$  s.d.

(EAGE) as an antigen to raise a rabbit polyclonal anti-peptide antibody (referred to as the anti-EAGE2 antibody), and confirmed that anti-EAGE2 antibody inhibited the trafficking of VSVGs045 (supplementary material Fig. S8).

At first, we used FRAP to monitor the transport of GFP-p58 from the ERGIC to the ER in semi-intact CHO-p58 cells. In the absence of the dominant negative form of Sar1, the extent of fluorescence recovery in the ER network after photobleaching was very small, probably because the rate of recycling of GFP-p58 is very fast (Fig. 5A,B, cytosol). Therefore, we could not analyze the effect of the anti-EAGE2 antibody or that of the various peptides derived from the N-terminal region of Yip1A on the retrograde transport of GFP-p58 (F.K., unpublished). However, in the presence of Sar1T39N, we could detect a significant increase in fluorescence recovery at the ER and a substantial inhibitory effect of the anti-EAGE2 antibody on the transport (Fig. 5A). The Yip1A peptides did not show any negative effects on the retrograde trafficking of p58 (Fig. 5B).

Owing to the fact that the deviations in FRAP data were very large, we estimated the retrograde transport of GFP-p58 in semi-intact CHO-p58 cells morphologically. Semi-intact CHO-p58 cells were incubated with cytosol and ATP with or without the addition of 5  $\mu$ g Sar1T39N at 32°C for 1 hour, and subsequently fixed and observed by confocal microscopy. After the incubation, in the presence of cytosol and ATP with Sar1T39N (Fig. 5C, Sar1T39N), almost all of the p58 protein had relocated to the ER network. Next,

we examined the effect of the anti-EAGE2 antibody on the retrograde transport of GFP-p58 in semi-intact cells. As shown in Fig. 5B (Sar1T39N+EAGE), the percentage of cells, in which GFP-p58 localized to the ER, decreased to approximately 38% of the control, which indicated that  $\beta$ COP was involved in the retrograde transport of p58. In the presence of a control antibody (normal rabbit IgG), transport of GFP-p58 was unaffected (Fig. 5D, Sar1T39N+rlgG). We also examined the effect of the anti-EAGE2 antibody on the retrograde transport of GT-GFP in the presence of Sar1T39N. As expected, the antibody did not inhibit the COPI-independent transport of GT-GFP (Fig. 5D, GT-GFP, Golgi→ER). These results indicate that the relocation of GFP-p58 to the ER is dependent on Sar1T39N and COPI, which was consistent with the results of previous studies that used intact cells (Girod et al., 1999). Using the retrograde transport assay for p58 described above, we found that peptides encoding Yip1-56, 1-109 and 57-109 did not inhibit the retrograde transport of p58 to the ER (Fig. 5E).

Taken together, these results indicated that Yip1A was involved in the COPI-independent retrograde transport of GT-GFP, but had no effect on the COPI-dependent transport of GFP-p58, as shown using semi-intact cell assays.

## Discussion

Yip1A belongs to the Yip family of proteins, which contain the Yip domain, and is thought to have a role in membrane trafficking. The localization of Yip1A has been controversial. In yeast, Yip1p is

reported to be localized to the Golgi and is essential for ER-to-Golgi transport (Yang et al., 1998). In mammalian cells, Yip1A is reported to localize to the ERES and the Golgi complex (Tang et al., 2001) or to the ERGIC (Yoshida et al., 2008). It has been reported that the cytosolic N-terminal domain of Yip1A binds to Sec23 or Sec24 and its overexpression blocks VSVG transport (Tang et al., 2001). In this study, we first raised an antibody against Yip1A that could be used for immunostaining of the endogenous protein to examine the precise localization of Yip1A. Several morphological assays revealed that Yip1A specifically colocalized with ERGIC53, which is a marker protein for the ERGIC (Fig. 1). However, we also found that Yip1A regulated the membrane association of Rab6 (Fig. 3), which localizes to the late Golgi or TGN (Goud et al., 1990; Antony et al., 1992). We cannot exclude the possibility that Yip1A relocates transiently to the late Golgi or TGN and functions there.

Previously, we reported that Yip1A-GFP is dispersed throughout the ER but is concentrated at the ERES in CHO-Yip cells, a stable cell line that expresses Yip1A-GFP (Kano et al., 2004). We observed that the punctate structures in which Yip1A-GFP accumulated sometimes jumped between one ER tubule and another, but were never targeted to the Golgi complex. We hypothesized that the different localization of Yip1A-GFP and endogenous Yip1A might be due to the effect of the protein tag. To compare the effect of different tags on Yip1A localization, we expressed GFP- or HA-tagged Yip1A in CHO cells and examined their localization. We found that HA-Yip1A was present in perinuclear structures and punctate structures, which corresponded to the ERGIC, whereas Yip1A-GFP was found in the ER and the ERES, but not in the Golgi, as previously reported. This indicated that the addition of protein tags could easily lead to the perturbation of Yip1A localization. Therefore, the protein tag that is used to investigate Yip1A function needs to be selected carefully.

Yoshida and colleagues (Yoshida et al., 2008) demonstrated that knockdown of YIPF5 (Yip1A), induced the partial Golgi disruption but did not affect anterograde transport of VSVG and soluble protein secretion. From these results, they supposed the possibility that the knockdown of Yip1A reduced fusion of retrograde vesicles budded from the ERGIC or the *cis*-Golgi to the ERGIC or the ER, so that net flow of membranes and Golgi-resident proteins back to the Golgi complex is reduced resulting in shrinkage and fragmentation of the Golgi without affecting the anterograde protein transport. However, there is a discrepancy between their results and ours about the Golgi morphology in Yip1A-knockdown cells. They found that the Golgi was partially fragmented in about 26% of the Yip1A-knockdown cells. In our study, we could not detect any significant morphological changes in the Golgi complex, or even any changes in the distribution of  $\beta$ COP, in Yip1A-knockdown cells. In our HeLa cell line, approximately 19% of cells in control and Yip1A-knockdown cells contained partially disrupted Golgi complex. Changes in the morphology of the Golgi during the cell cycle in mammalian cells are fairly common. Therefore it was difficult for us to evaluate precisely the extent of disruption of the Golgi that was induced by Yip1A knockdown in this study. In addition, we used a different siRNA for Yip1A knockdown. The difference in the extent of knockdown might lead to the different results in the Golgi morphology.

Using the transport assays, we found that Yip1A is involved in COPI-independent retrograde transport from the Golgi to the ER. In addition, a recombinant protein that consisted of the N-terminal portion (amino acids 1-56 or 1-109) of Yip1A fused to GST inhibited retrograde transport, but had no effect on anterograde transport (Fig.

4C) or the retrograde transport of GFP-p58 from the ERGIC to the ER (Fig. 5). The inhibition of retrograde transport was also confirmed by the knockdown of Yip1A in intact HeLa cells. Gene silencing of Yip1A by RNAi delayed the retrograde transport of Stx from the Golgi to the ER (Fig. 2C,D), but not the anterograde transport of VSVG (Fig. 2A,B), nor the retrograde transport of GFP-CI-MPR from endosomes to the Golgi (supplementary material Fig. S3). This paper is the first report that demonstrates the involvement of Yip1A in COPI-independent retrograde transport from the Golgi to the ER. It was an unexpected result because there have been many reports that show a possible involvement of Yip1A in anterograde transport. For example, Yip1A is known to bind to Sec23 and Sec24 (Tang et al., 2001), which are components of COPII vesicles that are required for vesicle budding from the ER, and overexpression of the N-terminal peptide of Yip1A leads to the inhibition of VSVG transport at the ER-Golgi interface. Yang and co-workers (Yang et al., 1998) reported that a yeast Yip1 mutant shows defects in secretion and an accumulation of ER membranes. Others have also demonstrated that Yip1p functions at an early stage in ER vesicle budding (Barrowman et al., 2003; Heidtman et al., 2003). On the contrary, we found that VSVG transport from the ER to the plasma membrane via the Golgi complex occurred normally in Yip1A-knockdown cells (Fig. 2B), and GST-tagged Yip1-56 or 1-109 did not inhibit the anterograde transport of GT-GFP (Fig. 4C). One possible explanation for the discrepancy between our results and others is that Yip1A might need to bind to COPII components to be delivered to the ERGIC, possibly as a cargo. Therefore, overexpression of the N-terminal domain of Yip1A might inhibit the budding of vesicles that contain VSVG, and thus result in the inhibition of its transport. In addition, the Yip family is conserved in eukaryotes including *Saccharomyces cerevisiae*, which lacks the ERGIC, and mammalian cells, which show distinct ERGIC clusters. Therefore Yip1A, which is localized to the ERGIC in mammalian cells, might be involved in other functions in addition to mediating the early steps of anterograde transport from the ER.

As shown in Fig. 2D, knockdown of Yip1A delayed the retrograde transport of Stx, but did not completely inhibit its transport. This suggests that Yip1A might not be an essential factor, but rather a regulator of the retrograde transport. However, we could not rule out the possibility that the small amount of Yip1A that remained in the Yip1A-knockdown cells was sufficient to drive the retrograde transport in a delayed manner. We surmised that one step that could be regulated by Yip1A was the membrane association of Rab6, which is known to be involved in COPI-independent retrograde transport from the Golgi to the ER. In this study, we showed that Rab6 dissociated from the Golgi membrane in Yip1A-knockdown HeLa cells (Fig. 3). Western blotting analysis also demonstrated that the amount of membrane-associated Rab6 in these cells decreased to approximately 50% of that in the control cells, and immunofluorescence studies revealed that a substantial amount of Rab6 dissociated from the Golgi complex into the cytoplasm in Yip1A-knockdown cells (Fig. 3C).

Grigoriev and colleagues (Grigoriev et al., 2007) reported that Rab6 regulates exocytic transport by enhancing the processive kinesin-dependent movement of secretory vesicles from the Golgi to the plus-ends of microtubules. They demonstrated that the secretion of VSVG was delayed, but not completely abolished, in Rab6-knockdown cells. We found that Yip1A knockdown reduced the amount of Golgi-associated Rab6. These results suggest that anterograde transport of VSVG should be delayed in Yip1A-knockdown cells, in which Rab6

has dissociated from the Golgi membranes. However, VSVG was transported normally from the ER to the plasma membrane via the Golgi in Yip1A-knockdown cells (Fig. 2B) and Yip1A seemed rather to be involved in retrograde transport from the Golgi to the ER (Fig. 2D). We suppose that the discrepancy is due to a difference in the amount of Rab6 in their experiments and ours. In the paper by Grigoriev et al. (Grigoriev et al., 2007), Rab6 was depleted by at least 90% upon RNAi. In our study, the total amount of Rab6 did not change, but approximately 50% of the Golgi-associated Rab6 was dissociated from the Golgi membrane in the Yip1A-knockdown cells compared with the control cells. The retention of 50% of the Golgi-associated Rab6 might be sufficient for VSVG transport in Yip1A-knockdown cells. Another possibility is that VSVG transport might be dependent on vesicle-associated Rab6, but not on Golgi-associated Rab6. Grigoriev et al. (Grigoriev et al., 2007) showed that Rab6 is present on exocytotic vesicles and directs the targeting of secretory vesicles to the plasma membrane. Therefore, Rab6 that is associated with the exocytotic vesicles might be responsible for controlling VSVG trafficking, and Rab6 on the Golgi membranes might have a different function. However, we could not rule out the possibility that the different subtypes of Rab6 have different functions, and that the subtype of Rab6 that was depleted in their paper (Grigoriev et al., 2007) is different from that of the Rab6 that was dissociated from the Golgi by Yip1A knockdown in our study. There are three subtypes of Rab6: Rab6A, Rab6A' and Rab6B. Rab6A and Rab6A' are expressed in HeLa cells, but Rab6B is expressed specifically in brain and is absent from HeLa cells (Opdam et al., 2000). Because of the high similarity in amino acid sequence between Rab6A and Rab6A', we could not identify the precise Rab6 isoforms that dissociated from the Golgi in Yip1A-knockdown cells. Specific antibodies against the Rab6 isoforms will allow us to define the specific function of each individual isoform.

An interaction between Rab proteins and Yip1A is plausible because the Yip family is considered to act as a regulator of Rab GTPase function. Indeed, Sivars et al. (Sivars et al., 2003) reported that mammalian Yip3, a member of the Yip family, dissociates the complex between Rab9 and Rab-GDI and thus enables Rab9 to bind to endosomal membranes. In addition, Calero and co-workers (Calero et al., 2003) reported that Yip1A could interact with yeast Rab6 in yeast. However, it is difficult to assume that Yip1A is a direct membrane receptor for Rab6 for the following reasons. First, we could not detect any interaction between Rab6 and Yip1A in vitro or in vivo by immunoprecipitation. We expressed HA- or Myc-tagged Yip1A or Rab6 proteins in HeLa cells and performed co-immunoprecipitation experiments. We also made GST-tagged recombinant proteins and examined the direct interaction of GST-Yip1A and GST-Rab6 in vitro. Unfortunately, however, we could not detect any interaction between them. Second, the localization of Rab6 and Yip1A was not identical. We could not perform dual immunostaining of Yip1A and Rab6 because the antibodies against both these proteins were produced in rabbits. Therefore, we expressed GFP-tagged Rab6 in HeLa cells and examined the colocalization of Yip1A and Rab6 in these cells. This revealed that GFP-Rab6 and Yip1A did not completely colocalize, although they were adjacent to each other (F.K., unpublished). Third, we could detect, both biochemically and morphologically, a substantial dissociation of Rab6 into the cytoplasm in Yip1A-knockdown cells, but complete dissociation was not observed. At present, we cannot discriminate whether Yip1A functions transiently or partially in the late Golgi or TGN as a direct receptor for Rab6, or whether Yip1A could regulate the localization of Rab6 via other Golgi-associated

protein factors, which remain to be identified. In support of the latter, the intracellular localization of Rab proteins is not perturbed in *yip3Δ* or *rtn1Δ* mutants in yeast (Geng et al., 2005). Further studies are needed to identify these factors.

In this study, a novel function of Yip1A as a regulator of retrograde transport from the Golgi to the ER was revealed. Finding the binding partners of Yip1A might help to elucidate the precise molecular mechanisms by which Yip1A functions in the transport. Our transport assay would be suitable for examining the functions of binding partner in the retrograde transport.

## Materials and Methods

### Cells

CHO-GT8 cells, which constitutively express a protein that comprises amino acids 1-60 of galactosyltransferase fused with GFP (GT-GFP) (Kano et al., 2000), were maintained as described previously (Kano et al., 2000; Kano et al., 2004). We established and maintained the CHO-p58 cells, which express GFP-tagged p58, according to the same protocol as for the CHO-GT8 cells. HeLa cells were maintained in DMEM supplemented with 10% FCS and penicillin-streptomycin (Gibco).

### Reagents and antibodies

GTP, ATP, creatine phosphate, creatine kinase, and protease inhibitors (antipain, chymostatin, pepstatin A, and leupeptin) were obtained from Sigma. Propidium iodide was purchased from Molecular Probes. ER tracker Blue-White DPX was purchased from Invitrogen. Other reagents were purchased from Wako Chemicals. The following antibodies were used: mouse monoclonal anti-βCOP antibody (clone maD; Sigma), rabbit polyclonal antibodies against Rab6 (C-19) and Rab1b (Santa Cruz Biotechnology), mouse monoclonal anti-Rab33b antibody (Frontier Science), rabbit anti-mannosidase II antibody (Chemicon), mouse monoclonal anti-GAPDH antibody (Chemicon), mouse monoclonal anti-GM130 antibody, anti-p230 antibody, and anti-p115 antibody (BD Transduction Laboratories), mouse anti-HSP47 antibody (Stressgen), mouse anti-Sec31A antibody (BD Transduction Laboratories). The mouse anti-ERGIC53 antibody was a gift from Hans-Peter Hauri (University of Basel, Basel, Switzerland). The polyclonal antibodies against Yip1A, YIPN and B8460, were raised in rabbits that had been immunized with a Yip1A peptide (FYQTSYSIDEQSQ and YSKQYAGYDYSQQGRFVPPD, respectively) by standard procedures (Scrum, Japan or Multiple Peptide Systems, San Diego, CA). The polyclonal antibody against βCOP (EAGE2) was prepared as described (Duden et al., 1991).

### Plasmids

The construct for GFP-tagged VSVGts045 was a gift from Jennifer Lippincott-Schwartz (National Institutes of Health, Bethesda, MD). To synthesize the GFP-p58 construct, a cDNA fragment that encoded enhanced GFP (EGFP) was inserted between the nucleotides that encoded the signal peptide (MAVSRRRRGPQAGAQSFFCALLLSFSQFVGS) and the subsequent amino acids of rat p58, which had been amplified from a rat brain cDNA library by PCR, in the mammalian expression vector, pCI-neo (Promega).

### RNAi

A small interfering RNA (siRNA) against human Yip1A (Ambion, ID 127564) or a scrambled siRNA (Ambion) was transfected into HeLa cells using Lipofectamine 2000 (Invitrogen) according to the manufacturer's instructions.

### Assay to measure the retrograde transport of Shiga toxin 1

Cy2-labelled Stx (Stx-Cy2) was prepared as described previously (Nishikawa et al., 2006). Shiga toxin 1 (Stx1) is produced by enterohemorrhagic *Escherichia coli*, and is identical to Shiga toxin produced by *Shigella dysenteriae*. Semi-confluent HeLa cells that had been transfected with siRNAs were placed on ice for 5 minutes, and then incubated with 1 μg/ml Stx-Cy2 on ice for 30 minutes. After washing twice with PBS, pre-warmed medium was added to the cells and they were incubated for the indicated times. The cells were then fixed and observed using a confocal microscope. We defined the cells in which Stx-Cy2 had accumulated in juxtanuclear structures as containing Stx-Cy2 in the Golgi, cells that showed the clear appearance of the toxin in the nuclear envelope and cytoplasmic reticular structures as containing Stx-Cy2 in the ER, and cells in which Stx-Cy2 was scattered in cytoplasmic punctate structures as containing the toxin in other organelles such as endosomes. We counted the number of cells that contained Stx-Cy2 in these locations. For all experiments, three independent transport assays were performed, and the percentages of cells in which Stx-Cy2 was in the Golgi or the ER are shown.

### Assay to measure the anterograde transport of GFP-tagged VSVGts045

48 hours after transfection with the Yip1A or control siRNA, the plasmid encoding GFP-tagged VSVGts045 was transfected into the cells. The cells were incubated at



39°C for 24 hours to allow the accumulation of the VSVG protein within the ER, and subsequently incubated at 32°C for the indicated times to induce the transport of VSVG from the ER. The cells were divided into three classes upon examination under the microscope. The first class comprised cells in which VSVGt045-GFP was present only in the ER network, i.e. the VSVG was localized to a reticular network throughout the cytoplasm; the second corresponded to cells in which VSVG accumulated in the juxtannuclear structures; and the third, cells in which VSVG appeared at filopodia or lamellipodia. The number of cells in each class was counted. Cells in which VSVGt045-GFP was present in both the ER and the Golgi were assigned to the second class. Then, we calculated the percentage of cells in which VSVGt045-GFP was localized to the ER, the Golgi, or the plasma membrane. For all experiments, three independent transport assays were performed, and the means and standard deviations were plotted.

### Measurement of the anterograde and retrograde transport of GT-GFP

Semi-confluent CHO-GT8 cells were treated with 10 µg/ml cycloheximide (CHX) at 37°C for 30 minutes to inhibit protein synthesis. The CHO-GT8 cells were then permeabilized with streptolysin O (SLO) as described (Kano et al., 2000). In our semi-intact cell assays, we identified individual semi-intact cells whose nuclei were stained with propidium iodide (PI) by light microscopy. PI is a membrane-impermeable nucleotide dye. We used PI as a marker for permeabilization of the semi-intact cells. The semi-intact CHO-GT8 cells were added to a reaction mixture that contained cytosol (protein concentration: 2.5–3.0 mg/ml), an ATP-regenerating system (1 mM ATP, 8 mM creatine kinase and 50 µM creatine phosphate), 1 mM GTP, 1 mg/ml glucose, and 10 µg/ml CHX, and the sample was placed on the stage of an LSM510 confocal microscope that was equipped with a temperature control unit (Zeiss). Cytosol from L5178Y cells was prepared as described (Kano et al., 2000). Rat liver cytosol was a gift from Masao Sakaguchi (University of Hyogo, Japan). An image of the whole cell was first obtained at low laser power. For the retrograde transport assay, the gain was increased because the GT-GFP signal in the ER was relatively weak. The focal plane was adjusted in order that the Golgi was clearly defined for the anterograde transport assay or the ER for the retrograde transport assay. At least one image was taken at imaging power (1% laser power) before bleaching to allow the steady-state distribution of GT-GFP to be quantified. Fluorescence within the Golgi or ER region was then almost completely bleached by scanning through successive focal planes at maximum laser power. The recovery of fluorescence within the Golgi (or ER) region was monitored by imaging, at 1% laser power, in the originally selected focal plane every 5 seconds for at least 10 minutes, or at 10 minutes. No significant photobleaching of GT-GFP was observed over the time course of the experiments. We arbitrarily assigned the average intensity of fluorescence in a selected region of the Golgi (or ER) in the prebleached cells as 100% and in the bleached cells as 0%. For all experiments, three independent transport assays were performed, and the means and s.d. were plotted.

### Recombinant proteins

To produce recombinant mouse Yip1A polypeptides as glutathione S-transferase (GST) fusion proteins, cDNA fragments that encoded the N-terminal domain of mouse Yip1A (amino acids 1–56, 1–109 or 57–109) were amplified by PCR from a mouse brain cDNA library and subcloned into the *Xho*I site of pGEX-5X-1 (GE Healthcare). GST-tagged Yip1A peptides were purified according to the method as described (Kihara et al., 2008). Recombinant dominant negative mutant Sar1T39N were prepared as described (Rowe and Balch, 1995).

### Assay to measure the retrograde transport of GFP-p58

Semi-confluent CHO-p58 cells were permeabilized using SLO, and incubated with rat liver cytosol (protein concentration: 2.5–3.0 mg/ml), 5 µg recombinant Sar1T39N protein, and the indicated antibodies or proteins at 32°C for 1 hour. After washing with TB, the cells were fixed and observed using a confocal microscope. We counted the number of cells in which GFP-p58 had relocated completely to the ER. Three independent experiments were performed and the means and s.d. for the percentages of cells in which GFP-p58 was localized to the ER are shown in the graph. For FRAP assay, the fluorescence recovery within the bleached ER region in CHO-p58 cells was monitored in the same way as the retrograde transport assay of GT-GFP.

This work was supported by PRESTO from Japan Science and Technology Agency (F.K.), Grant-in-Aid for Young Scientists (B) (F.K.), and Grant-in-Aid for Exploratory Research (MM: 19657057) from Japan Society for the Promotion of Science.

### References

Allan, B. B., Moyer, B. D. and Balch, W. E. (2000). Rab1 recruitment of p115 into a cis-SNARE complex: programming budding COPII vesicles for fusion. *Science* **289**, 444–448.

Altan-Bonnet, N., Sougrat, R., Liu, W., Snapp, E. L., Ward, T. and Lippincott-Schwartz, J. (2006). Golgi inheritance in mammalian cells is mediated through endoplasmic reticulum export activities. *Mol. Biol. Cell* **17**, 990–1005.

Antony, C., Cibert, C., Géraud, G., Santa Maria, A., Maro, B., Mayau, V. and Goud, B. (1992). The small GTP-binding protein rab6p is distributed from medial Golgi to the trans-Golgi network as determined by a confocal microscopic approach. *J. Cell Sci.* **103**, 785–796.

Barrowman, J., Wang, W., Zhang, Y. and Ferro-Novick, S. (2003). The Yip1p.Yif1p complex is required for the fusion competence of endoplasmic reticulum-derived vesicles. *J. Biol. Chem.* **278**, 19878–19884.

Bremser, M., Nickel, W., Schweikert, M., Ravazzola, M., Amherdt, M., Hughes, C. A., Söllner, T. H., Rothman, J. E. and Wieland, F. T. (1999). Coupling of coat assembly and vesicle budding to packaging of putative cargo receptors. *Cell* **96**, 495–506.

Calero, M., Winand, N. J. and Collins, R. N. (2002). Identification of the novel proteins Yip4p and Yip5p as Rab GTPase interacting factors. *FEBS Lett.* **515**, 89–98.

Calero, M., Chen, C. Z., Zhu, W., Winand, N., Havas, K. A., Gilbert, P. M., Burd, C. G. and Collins, R. N. (2003). Dual prenylation is required for Rab protein localization and function. *Mol. Biol. Cell* **14**, 1852–1867.

Chen, C. Z. and Collins, R. N. (2005). Insights into biological functions across species: examining the role of Rab proteins in YIP1 family function. *Biochem. Soc. Trans.* **33**, 614–618.

Duden, R., Griffiths, G., Frank, R., Argos, P. and Kreis, T. E. (1991). Beta-COP, a 110 kd protein associated with non-clathrin-coated vesicles and the Golgi complex, shows homology to beta-adaptin. *Cell* **64**, 649–665.

Gaynor, E. C., Graham, T. R. and Emr, S. D. (1998). COPI in ER/Golgi and intra-Golgi transport: do yeast COPI mutants point the way? *Biochim. Biophys. Acta* **1404**, 33–51.

Geng, J., Shin, M. E., Gilbert, P. M., Collins, R. N. and Burd, C. G. (2005). Saccharomyces cerevisiae Rab-GDI displacement factor ortholog Yip3p forms distinct complexes with the Ypt1 Rab GTPase and the reticulon Rtn1p. *Eukaryot. Cell* **4**, 1166–1174.

Girod, A., Storrer, B., Simpson, J. C., Johannes, L., Goud, B., Roberts, L. M., Lord, J. M., Nilsson, T. and Pepperkok, R. (1999). Evidence for a COP-1-independent transport route from the Golgi complex to the endoplasmic reticulum. *Nat. Cell Biol.* **1**, 423–430.

Goud, B., Zahraoui, A., Tavitian, A. and Saraste, J. (1990). Small GTP-binding protein associated with Golgi cisternae. *Nature* **345**, 553–556.

Grigoriev, I., Splinter, D., Keijzer, N., Wulf, P. S., Demmers, J., Ohtsuka, T., Modesti, M., Maly, I. V., Grosveld, F., Hoogenraad, C. C. et al. (2007). Rab6 regulates transport and targeting of exocytotic carriers. *Dev. Cell* **13**, 305–314.

Grosshans, B. L., Ortiz, D. and Novick, P. (2006). Rabs and their effectors: achieving specificity in membrane traffic. *Proc. Natl. Acad. Sci. USA* **103**, 11821–11827.

Hammond, A. T. and Glick, B. S. (2000). Dynamics of transitional endoplasmic reticulum sites in vertebrate cells. *Mol. Biol. Cell* **11**, 3013–3030.

Heidtmann, M., Chen, C. Z., Collins, R. N. and Barlowe, C. (2003). A role for Yip1p in COPII vesicle biogenesis. *J. Cell Biol.* **163**, 57–69.

Hidalgo, J., Muñoz, M. and Velasco, A. (1995). Trimeric G proteins regulate the cytosol-induced redistribution of Golgi enzymes into the endoplasmic reticulum. *J. Cell Sci.* **108**, 1805–1815.

Hirosako, K., Imasato, H., Hirota, Y., Kuronita, T., Masuyama, N., Nishioka, M., Umeda, A., Fujita, H., Himeno, M. and Tanaka, Y. (2004). 3-Methyladenine specifically inhibits retrograde transport of cation-independent mannose 6-phosphate/insulin-like growth factor II receptor from the early endosome to the TGN. *Biochem. Biophys. Res. Commun.* **316**, 845–852.

Jiang, S. and Storrer, B. (2005). Cisternal rab proteins regulate Golgi apparatus redistribution in response to hypotonic stress. *Mol. Biol. Cell* **16**, 2586–2596.

Jin, C., Zhang, Y., Zhu, H., Ahmed, K., Fu, C. and Yao, X. (2005). Human Yip1A specifies the localization of Yif1 to the Golgi apparatus. *Biochem. Biophys. Res. Commun.* **334**, 16–22.

Kano, F., Sako, Y., Tagaya, M., Yanagida, T. and Murata, M. (2000). Reconstitution of brefeldin A-induced golgi tubulation and fusion with the endoplasmic reticulum in semi-intact chinese hamster ovary cells. *Mol. Biol. Cell* **11**, 3073–3087.

Kano, F., Tanaka, A. R., Yamauchi, S., Kondo, H. and Murata, M. (2004). Cdc2 kinase-dependent disassembly of endoplasmic reticulum (ER) exit sites inhibits ER-to-Golgi vesicular transport during mitosis. *Mol. Biol. Cell* **15**, 4289–4298.

Kihara, T., Kano, F. and Murata, M. (2008). Modulation of SRF-dependent gene expression by association of SPT16 with MKL1. *Exp. Cell Res.* **314**, 629–637.

Kuge, O., Dascher, C., Orci, L., Rowe, T., Amherdt, M., Plutner, H., Ravazzola, M., Tanigawa, G., Rothman, J. E. and Balch, W. E. (1994). Sar1 promotes vesicle budding from the endoplasmic reticulum but not Golgi compartments. *J. Cell Biol.* **125**, 51–65.

Lawe, D. C., Sitouah, N., Hayes, S., Chawla, A., Virbasius, J. V., Tuft, R., Fogarty, K., Lifshitz, L., Lambright, D. and Corvera, S. (2003). Essential role of Ca2+/calmodulin in Early Endosome Antigen-1 localization. *Mol. Biol. Cell* **14**, 2935–2945.

Lowe, M. and Barr, F. A. (2007). Inheritance and biogenesis of organelles in the secretory pathway. *Nat. Rev. Mol. Cell Biol.* **8**, 429–439.

Miles, S., McManus, H., Forsten, K. E. and Storrer, B. (2001). Evidence that the entire Golgi apparatus cycles in interphase HeLa cells: sensitivity of Golgi matrix proteins to an ER exit block. *J. Cell Biol.* **155**, 543–555.

Nishikawa, K., Watanabe, M., Kita, E., Igai, K., Omata, K., Yaffe, M. B. and Natori, Y. (2006). A multivalent peptide library approach identifies a novel Shiga toxin inhibitor that induces aberrant cellular transport of the toxin. *FASEB J.* **20**, 2597–2599.

Opdam, F. J., Echarat, A., Croes, H. J., van den Hurk, J. A., van de Vorstenbosch, R. A., Ginsel, L. A., Goud, B. and Fransen, J. A. (2000). The small GTPase Rab6B, a novel Rab6 subfamily member, is cell-type specifically expressed and localised to the Golgi apparatus. *J. Cell Sci.* **113**, 2725–2735.

Pepperkok, R., Scheel, J., Horstmann, H., Hauri, H. P., Griffiths, G. and Kreis, T. E. (1993). Beta-COP is essential for biosynthetic membrane transport from the endoplasmic reticulum to the Golgi complex *in vivo*. *Cell* **74**, 71–82.

- Plutner, H., Cox, A. D., Pind, S., Khosravi-Far, R., Bourne, J. R., Schwaninger, R., Der, C. J. and Balch, W. E. (1991). Rab1b regulates vesicular transport between the endoplasmic reticulum and successive Golgi compartments. *J. Cell Biol.* **115**, 31-43.
- Rowe, T. and Balch, W. E. (1995). Expression and purification of mammalian Sar1. *Methods Enzymol.* **257**, 49-53.
- Saraste, J., Lahtinen, U. and Goud, B. (1995). Localization of the small GTP-binding protein rab1p to early compartments of the secretory pathway. *J. Cell Sci.* **108**, 1541-1552.
- Sato, K. and Nakano, A. (2007). Mechanisms of COPII vesicle formation and protein sorting. *FEBS Lett.* **581**, 2076-2082.
- Serafini, T., Orci, L., Amherdt, M., Brunner, M., Kahn, R. A. and Rothman, J. E. (1991). ADP-ribosylation factor is a subunit of the coat of Golgi-derived COP-coated vesicles: a novel role for a GTP-binding protein. *Cell* **67**, 239-253.
- Shakoori, A., Fujii, G., Yoshimura, S., Kitamura, M., Nakayama, K., Ito, T., Ohno, H. and Nakamura, N. (2003). Identification of a five-pass transmembrane protein family localizing in the Golgi apparatus and the ER. *Biochem. Biophys. Res. Commun.* **312**, 850-857.
- Sivars, U., Aivazian, D. and Pfeffer, S. R. (2003). Yip3 catalyses the dissociation of endosomal Rab-GDI complexes. *Nature* **425**, 856-859.
- Springer, S., Spang, A. and Schekman, R. (1999). A primer on vesicle budding. *Cell* **97**, 145-148.
- Storrie, B., White, J., Röttger, S., Stelzer, E. H., Sugauma, T. and Nilsson, T. (1998). Recycling of golgi-resident glycosyltransferases through the ER reveals a novel pathway and provides an explanation for nocodazole-induced Golgi scattering. *J. Cell Biol.* **143**, 1505-1521.
- Stroud, W. J., Jiang, S., Jack, G. and Storrie, B. (2003). Persistence of Golgi matrix distribution exhibits the same dependence on Sar1p activity as a Golgi glycosyltransferase. *Traffic* **4**, 631-641.
- Tang, B. L., Ong, Y. S., Huang, B., Wei, S., Wong, E. T., Qi, R., Horstmann, H. and Hong, W. (2001). A membrane protein enriched in endoplasmic reticulum exit sites interacts with COPII. *J. Biol. Chem.* **276**, 40008-40017.
- Tisdale, E. J., Bourne, J. R., Khosravi-Far, R., Der, C. J. and Balch, W. E. (1992). GTP-binding mutants of rab1 and rab2 are potent inhibitors of vesicular transport from the endoplasmic reticulum to the Golgi complex. *J. Cell Biol.* **119**, 749-761.
- Valsdottir, R., Hashimoto, H., Ashman, K., Koda, T., Storrie, B. and Nilsson, T. (2001). Identification of rabaptin-5, rabex-5, and GM130 as putative effectors of rab33b, a regulator of retrograde traffic between the Golgi apparatus and ER. *FEBS Lett.* **508**, 201-209.
- Ward, T. H., Polishchuk, R. S., Caplan, S., Hirschberg, K. and Lippincott-Schwartz, J. (2001). Maintenance of Golgi structure and function depends on the integrity of ER export. *J. Cell Biol.* **155**, 557-570.
- White, J., Johannes, L., Mallard, F., Girod, A., Grill, S., Reinsch, S., Keller, P., Tzschaschel, B., Echard, A., Goud, B. et al. (1999). Rab6 coordinates a novel Golgi to ER retrograde transport pathway in live cells. *J. Cell Biol.* **147**, 743-760.
- Yang, X., Matern, H. T. and Gallwitz, D. (1998). Specific binding to a novel and essential Golgi membrane protein (Yip1p) functionally links the transport GTPases Ypt1p and Ypt31p. *EMBO J.* **17**, 4954-4963.
- Yoshida, Y., Suzuki, K., Yamamoto, A., Sakai, N., Bando, M., Tanimoto, K., Yamaguchi, Y., Sakaguchi, T., Akhter, H., Fujii, G. et al. (2008). YIPF5 and YIF1A recycle between the ER and the Golgi apparatus and are involved in the maintenance of the Golgi structure. *Exp Cell Res.* **314**, 3427-3443.
- Zaal, K. J., Smith, C. L., Polishchuk, R. S., Altan, N., Cole, N. B., Ellenberg, J., Hirschberg, K., Presley, J. F., Roberts, T. H., Siggia, E. et al. (1999). Golgi membranes are absorbed into and reemerge from the ER during mitosis. *Cell* **99**, 589-601.
- Zheng, J. Y., Koda, T., Fujiwara, T., Kishi, M., Ikehara, Y. and Kakinuma, M. (1998). A novel Rab GTPase, Rab33B, is ubiquitously expressed and localized to the medial Golgi cisternae. *J. Cell Sci.* **111**, 1061-1069.